874–888 *Nucleic Acids Research, 2011, Vol. 39, No. 3* *Published online 4 October 2010*
doi:10.1093/nar/gkq870

DNA methyltransferase 3b preferentially associates with condensed chromatin

Katsunobu Kashiwagi[1], Keisuke Nimura[1], Kiyoe Ura[1,2,*] and Yasufumi Kaneda[1,*]

[1]Division of Gene Therapy Science, Osaka University Graduate School of Medicine, 2-2 Yamada-oka, Suita, Osaka 565-0871 and [2] PRESTO, Japan Science and Technology Agency (JST), Kawaguchi, Saitama 332-0012, Japan

Received September 18, 2009; Revised September 3, 2010; Accepted September 15, 2010

ABSTRACT

In mammals, DNA methylation is catalyzed by DNA methyltransferases (DNMTs) encoded by *Dnmt1*, *Dnmt3a* and *Dnmt3b*. Since, the mechanisms of regulation of Dnmts are still largely unknown, the physical interaction between Dnmt3b and chromatin was investigated *in vivo* and *in vitro*. In embryonic stem cell nuclei, Dnmt3b preferentially associated with histone H1-containing heterochromatin without any significant enrichment of silent-specific histone methylation. Recombinant Dnmt3b preferentially associated with nucleosomal DNA rather than naked DNA. Incorporation of histone H1 into nucleosomal arrays promoted the association of Dnmt3b with chromatin, whereas histone acetylation reduced Dnmt3b binding *in vitro*. In addition, Dnmt3b associated with histone deacetylase SirT1 in the nuclease resistant chromatin. These findings suggest that Dnmt3b is preferentially recruited into hypoacetylated and condensed chromatin. We propose that Dnmt3b is a 'reader' of higher-order chromatin structure leading to gene silencing through DNA methylation.

INTRODUCTION

Methylation of cytosine C5 of CpG dinucleotides is a characteristic DNA modification in many eukaryotic genomes that plays an important role in gene silencing (1,2). In mammals, DNA methylation patterns change drastically during early development, and the establishment and maintenance of proper genomic DNA methylation is required for normal development (3–5). In somatic cells, 70–80% of all CpG dinucleotides are methylated (6). This epigenetic gene regulation plays an important role in X chromosome inactivation, genomic imprinting and stable silencing of retrotransposons (7–9). Covalent modification at the C5 position is mediated by DNA methyltransferases (Dnmts). Three active Dnmt genes, *Dnmt1*, *Dnmt3a* and *Dnmt3b*, have been identified in mammals (10,11). All three genes are essential for normal mouse development (12,13). However, it is not known how each Dnmt selects target CpG sites in the genome. Gene silencing in eukaryotes is mediated by a variety of epigenetic phenomena in addition to DNA methylation, including histone modification, chromatin remodeling and non-coding RNAs, and there is extensive cross-talk between these mechanisms (14–17). Histones function as structural components for packaging DNA in the nucleus but are also key regulators of gene expression (18). Various post-translational histone modifications, including acetylation, methylation, phosphorylation, ubiquitination and sumoylation, and other histone variants serve as functional codes that dictate the recruitment of protein complexes or change higher-order chromatin structure to achieve gene activation or inactivation (19–21). Histone H3 lysine 9 (H3K9) is trimethylated in heterochromatin, and mutation of the histone H3K9-specific methyltransferase causes a loss of genomic DNA methylation in *Neurospora crassa* (22,23), *Arabidopsis thaliana* (24) and mouse cells (25), which suggests that DNA methylation acts downstream from histone H3K9 methylation. In human cells, DNMT3B physically associates with the histone H3K27-specific methyltransferase Enhancer of Zest homolog 2 (EZH2), a member of the Polycomb group of proteins, and targets specific genes depending on its histone methyltransferase activity (26). In addition, recent data indicate that Dnmt3a is recruited to symmetric methylation of histone H4 arginine 3 mediated by the histone arginine methyltransferase PRMT5 (27). Conversely, Dnmt3L, which lacks conserved residues known to be involved in Dnmt activity (28) but interacts with Dnmt3 proteins to stimulate DNA methylation activity (29–31), binds to the N-terminus of histone H3,

*To whom correspondence should be addressed. Tel: +81 6 6879 3906; Fax: +81 6 6879 3909; Email: kiyoeura@gts.med.osaka-u.ac.jp
*Correspondence may also be addressed to Yasufumi Kaneda. Tel: +81 6 6879 3901; Fax: +81 6 6879 3909; Email: kaneday@gts.med.osaka-u.ac.jp

and this binding is inhibited by methylation of histone H3K4 (32). Crystallographic and biochemical studies revealed the specific interaction of the ATRX-DNMT3-DNMT3L (ADD) domain of Dnmt3L and DNMT3A with unmethylated lysine 4 in the amino-terminal tail of histone H3 (32–34). Accumulating evidence suggests that there is extensive crosstalk between DNA methylation and histone modification. Aside from histone modifications, disruption of histone H1 genes affects DNA methylation in *A. thaliana* (35) and mouse ES cells (36), suggesting a functional link between DNA methylation and linker histone H1-dependent higher-order chromatin structure. Biochemical studies revealed that Dnmts interact with chromatin (32,37,38), however, it remains to be determined whether Dnmt itself recognizes specific histone modifications or higher-order chromatin structure. The current study characterized the association of two *de novo* methyltransferase, Dnmt3a2 and Dnmt3b, with nuclear chromatin in ES cells and reconstituted chromatin templates. In the nucleus, Dnmt3b, but not Dnmt3a2, preferentially associated with histone H1-containing chromatin without any significant enrichment of silent chromatin-specific modifications. We demonstrated the preferential interaction of Dnmt3b with nucleosomal DNA rather than naked DNA. In contrast to Dnmt3b, Dnmt3a2 bound weakly to all substrates regardless of DNA structure. The incorporation of histone H1 into nucleosomal arrays promoted the association of Dnmt3b, while histone acetylation reduced Dnmt3b binding *in vitro*. Consistent with these observations, the NAD^+-dependent histone deacetylase SirtT1, the mammalian homolog of yeast Sir2, which specifically deacetylates histone H4 lysine 16 (H4K16) (39,40), was enriched in Dnmt3b-associated chromatin in ES cell nuclei. These results provide molecular evidence that Dnmts differentially interact with higher-order chromatin. We propose that Dnmt3b specifically recognizes higher-order chromatin structures to induce DNA methylation of condensed chromatin.

MATERIALS AND METHODS

Cell culture and *in vitro* differentiation

Undifferentiated ES cells (ht7) were maintained in DMEM, as described earlier (41). To induce differentiation, ES cells were cultivated in suspension without leukemia inhibitory factor (LIF) to form embryoid body (EB) cells. Five days after induction, EB cells were plated in tissue culture dishes and cultured for an additional 5 days.

Preparation of nuclei

ES cell nuclei were prepared as described earlier, with some modifications (42,43). Briefly, ES cells were resuspended in Nuclei Isolation Buffer (NIB) containing 10 mM Tris–HCl (pH 7.5), 60 mM KCl, 15 mM NaCl, 1.5 mM $MgCl_2$, 1 mM $CaCl_2$, 0.25 M sucrose, 10% (v/v) glycerol, 1 mM dithiothreitol (DTT), 0.1 mM phenylmethylsulfonyl fluoride (PMSF) and EDTA-free protease inhibitor cocktail (Roche). Cells were resuspended in NIB containing 0.1% (v/v) Nonidet P-40 (NP40), allowed to swell for 10 min, and then homogenized with a Dounce homogenizer on ice. The nuclei were pelleted by centrifugation at 500*g* for 10 min at 4°C to remove the soluble protein (cytoplasmic fraction), washed with NIB, and then resuspended in the same buffer.

Cell fractionation

Cell fractionation was performed as described earlier with some modifications (44). After collecting the cytoplasmic fraction, as described above, nuclei were suspended in NIB, and DNA was measured by UV absorbance at 260 nm in saturated 5 M NaCl, 8 M Urea buffer (20 OD_{260} units corresponded to 1 mg/ml DNA) (43). The nuclear pellets were diluted to 1.5 mg/ml DNA in NIB. The nuclei were treated with 0.5 U/μl (333 U) of RNase-free DNaseI (Sigma) for 15 min at 37°C. Ammonium sulfate was added to a final concentration of 0.25 M and the samples were incubated for 10 min at 25°C. The solubilized chromatin (chromatin fraction) was collected by centrifugation at 5000*g* for 10 min at 4°C. The pellets were extracted again with 2 M NaCl in NIB and then incubated for 5 min at 4°C (2 M NaCl wash fraction). To remove the remaining DNA and histones, the samples were centrifuged at 5000*g* for 5 min at 4°C. The remaining pellets, which contained the nuclear matrix (nuclear matrix fraction), was solubilized in 8 M urea containing 0.1 M NaH_2PO_4, 10 mM Tris–HCl (pH 8.0), EDTA-free protease inhibitor cocktail and 0.1 mM PMSF.

Chromatin fractionation

Micrococcal nuclease (MNase) digestion was performed as described earlier, with some modifications (42,45,46). Briefly, the nuclei were isolated as described above. The nuclear pellets were suspended in NIB at a concentration of 1.5 mg/ml DNA, pre-incubated for 10 min at 30°C and treated with increasing amounts of MNase (5, 20 or 80 U/mg DNA, Worthington) for 10 min at 30°C. After incubation, the nuclei were rapidly cooled on ice for 10 min and then subjected to centrifugation at 12 800*g* for 10 min at 4°C. The supernatant (S1 fraction) was collected and the pellets were resuspended in 2 mM EDTA, and then incubated for 10 min on ice. Suspended pellets were subjected to centrifugation at 12 800*g* for 10 min at 4°C. The supernatant was collected (S2 fraction) and the pellets were resuspended in 2 mM EDTA (P fraction). The amount of DNA in each fraction was measured using Pico Green (Invitrogen), according to the manufacturer's instructions. Equivalent amounts of DNA (600 ng) were separated by SDS–PAGE and analyzed by immunoblot. For DNA analysis, aliquots from each fraction were treated with 20 μg/ml of RNase A for 1 h at 37°C and then 40 μg/ml of proteinase K overnight at 50°C. The DNA was extracted twice with a solution of phenol:chloroform:isoamyl alcohol (25:24:1) and precipitated with ethanol. The DNA was analyzed by 1.5% agarose gel electrophoresis in 1× TAE and visualized with SYBR-Green I (Invitrogen).

Establishment of a FLAG-Dnmt3b-expressing cell line

The full-length cDNA of Dnmt3b with FLAG sequences fused to the N-terminus was cloned into the pCAGIpuro expression vector (kindly provided by Dr H. Niwa, RIKEN Japan) to construct pCAG-FLAG-Dnmt3b-IRES-puro. To generate ES cells that stably expressed FLAG-tagged Dnmt3b, the expression vector was introduced into parental ES cells (ht7) by electroporation (Bio-Rad).

Purification of Dnmt3b-associated proteins and chromatin

Nuclear extracts (S2 fractions) were prepared from FLAG-Dnmt3b-expressing cells by incubating the cells on ice with nuclei extraction buffer (NEB) [10 mM Tris–HCl (pH 7.5), 2 mM EDTA, 10% (v/v) glycerol, 0.1 mM PMSF and EDTA-free protease inhibitor cocktail (Roche)] containing 400 mM NaCl (NEB400). Extracted nuclear pellets were subjected to centrifugation at 12 800*g* for 10 min at 4°C. The supernatant was collected (S2 fraction), and a one-third volume of NEB400 containing 0.3% (v/v) NP40 was added. The nuclear extract was incubated with pre-equilibrated FLAG-M2 agarose (Sigma) for 4 h at 4°C with rotation. The immunoprecipitates were washed three times with NEB400 containing 0.1% (v/v) NP40 for 10 min at 4°C with rotation. After washing, FLAG-Dnmt3b immunoprecipitates were eluted with 0.4 mg/ml FLAG-peptide in NEB400 containing 0.1% NP40 for 1 h at 4°C with rotation. The purified proteins were precipitated with acetone and separated on SDS–polyacrylamide gels. Protein bands stained with silver were excised from the gel, in-gel digested with trypsin and analyzed by LC–MS/MS.

To identify the histone modification specificity of Dnmt3b, nuclear extraction and immunoprecipitation were carried out in NEB containing 75 mM NaCl (NEB75) and NEB75 with 0.1% (v/v) NP40, respectively, as described above. For analysis of histone acetylation, nuclear extraction and immunoprecipitation were carried out in NEB containing 65 mM NaCl and 10 mM sodium butyrate (Na butyrate, NEB65B) and NEB65B with 0.1% (v/v) NP40, respectively, as described above. FLAG-M2 agarose was collected and the immunoprecipitates were extracted with Laemmli's sample buffer (47). SDS–PAGE was performed under standard conditions and the separated proteins were transferred to the nitrocellulose membrane (GE Healthcare). Membranes were probed with primary antibodies as describe below. Blots were then probed with HRP-conjugated secondary antibodies or probed with Alexa 633 anti-rabbit IgG (1:1000; Invitrogen A-21071). Dnmt3b-specific bound histone modification was determined by quantifying the intensity of the bands using a Typhoon PhosphorImager (GE Healthcare) and ImageQuant software (Molecular Dynamics).

Chromatin isolation and sucrose gradient sedimentation

ES cell nuclei were treated with MNase (20 U/mg DNA) and the S2 fraction was extracted at 4°C with nuclei extraction buffer (NEB75), as described above. The S2 fraction was applied to a 10–30% (w/v) sucrose gradient containing NEB75 and centrifuged for 3 h at 50 000 rpm at 4°C in a SW55 rotor (Beckman). After sedimentation, equal volumes of each sample were recovered from the top. Equivalent volumes from each fraction were separated by SDS–PAGE and analyzed by immunoblot. For DNA analysis, fractionated samples were extracted with phenol-chloroform-isoamyl alcohol and precipitated as described above.

Expression and purification of GST-Dnmt3a2 and GST-Dnmt3b

Full-length Dnmt3a2 and Dnmt3b cDNAs were introduced into pGEX-6P1 (GE Healthcare). *Escherichia coli* BL21 (DE3) were transformed with expression vectors and cultured as previously described with some modifications (48). Harvested bacteria were sonicated in buffer [PBS containing 330 mM NaCl, 0.1% (w/v) Triton X-100, 1 mM DTT and EDTA-free protease inhibitor cocktail (Roche)], and then centrifuged at 12000*g* for 10 min at 4°C. The supernatant was collected and filtered through a 0.45-μm Millex GV filter (Millipore). The filtered supernatant was loaded onto a GSTrap HP column (GE Healthcare) and eluted with 10 mM glutathione (reduced form) in sonication buffer. The eluted fractions were further purified by gel filtration chromatography using a HiLoad 16/60 Superdex 200 column (GE Healthcare) pre-equilibrated with gel filtration buffer G [10 mM Tris–HCl (pH 7.5), 1 mM DTT, 1 mg/ml antipain, 1 mg/ml aprotinin, 0.4 mg/ml pepstatin] plus 330 mM KCl. The main fractions were collected and dialyzed against buffer G containing 200 mM KCl, 10% glycerol and 0.5 mM DTT for 2 h, followed by buffer G containing 50 mM KCl, 10% glycerol and 0.5 mM DTT for 2 h. GSTrap HP and HiLoad 16/60 Superdex 200 columns were connected to an ÄKTA Explorer 100 FPLC System (GE Healthcare).

Reconstitution of 12-mer nucleosomal arrays

Hypo- and hyperacetylated core histones were isolated from HeLa cells and treated without or with 10 mM Na butyrate for 24 h, respectively (43). DNA templates containing 1, 4 and 12 tandem repeats of a 208-bp '601' sequence (49) were mixed with HeLa core histone proteins to reconstitute nucleosomes by salt dialysis, as described previously (43). The 208-bp 601 sequence consists of a strong nucleosome positioning sequence and contains 19 CpG sites. Core histone proteins were mixed with DNA in a 1:1 ratio in 2 M NaCl-10 mM Tris–HCl (pH 7.5), 1 mM EDTA (TE), followed by serial dialysis against 1 M NaCl-TE for 4 h, 0.75 M NaCl-TE for another 4 h, and finally TE overnight. The reconstitution quality was examined by Sca I digestion followed by 0.7% nucleoprotein agarose gel electrophoresis in 0.25× TBE, as described earlier (50). The gels were stained with SYBR Green I (Invitrogen) and analyzed using a FluorImager 595 (GE Healthcare).

Linker histone assembly with reconstituted nucleosomal arrays

Nucleosomal arrays were incubated with various amounts of histone H1, purified from HeLa cells, in binding buffer [10 mM Tris–HCl (pH 7.5), 1 mM EDTA, 50 mM KCl and 1 μg/μl BSA] overnight on ice (43). Samples were mixed with an equal volume of loading solution [10 mM Tris–HCl (pH 7.5), 1 mM EDTA, 50 mM KCl and 6% glycerol] and resolved by 0.7% nucleoprotein agarose gel electrophoresis in 0.25× TBE. To determine histone stoichiometry, histone H1-containing nucleosomal arrays were precipitated in binding buffer containing 10 mM $MgCl_2$, as previously described, with some modification (51,52). Briefly, precipitated nucleosomal arrays were washed in binding buffer without BSA five times, and then resuspended in Laemmli's sample buffer (47). Nucleosomal arrays were separated by SDS–PAGE and visualized by SYPRO-Orange (Invitrogen) staining. Histone stoichiometry was determined by quantifying the intensity of the bands using a FluorImager 595 (GE Healthcare) and ImageQuant software (Molecular Dynamics).

Micrococcal nuclease mapping

Reconstitited nucleosomal arrays (24.26 ng of DNA) in the absence or presence of histone H1 were digested with increasing amounts of MNase (0.141, 0.281, 0.562 and 1.125 U). Products of digestion were labeled with [γ-^{32} P]ATP and analyzed by native PAGE as described earlier (53).

Sedimentation velocity analysis of the nucleosomal arrays

Sedimentation velocity experiments were performed using a Beckman XL-I analytical ultracentrifuge equipped with scanner optics, as previously described (54). The initial sample absorbance at 260 nm was between 0.6 and 0.8. Samples (360 μl) were equilibrated in TE (pH 7.5) containing 2.5 mM NaCl at 20°C for 30 min in the analytical ultracentrifuge before sedimentation at 15 000 rpm. Using the UltraScan data analysis program (version 7.4), boundaries were analyzed by the method of van Holde and Weischet (54). Sedimentation coefficients were corrected to $S_{20,w}$ using a partial specific volume of 0.622 ml/g for saturated chromatin arrays (50).

In vitro binding assay

Various lengths of naked 601 DNA or reconstituted chromatin assembled with or without histone H1 were incubated with purified GST-Dnmt3a2 or GST-Dnmt3b for 1 h at room temperature in binding buffer [10 mM Tris–HCl (pH 7.5), 50 mM KCl, 1 mM EDTA, 5% glycerol, 0.25 mM DTT and EDTA-free protease inhibitor cocktail (Roche)]. After incubation, anti-GST antibody (MBL) was added to a final concentration of 0.025 mg/ml and the samples were incubated overnight at 4°C in 10 mM Tris–HCl (pH 7.5), 50 mM KCl, 1 mM EDTA, 1.25% glycerol, 0.0625 mM DTT and EDTA-free protease inhibitor cocktail. Pre-equilibrated Dynabeads Protein G (Dynal) was added, and the reaction mixture was incubated on ice for 1 h. Protein complexes were washed twice with 10 mM Tris–HCl (pH 7.5), 50 mM KCl, 1 mM EDTA and EDTA-free protease inhibitor cocktail, and collected by magnetic separation according to the manufacturer's instructions. Collected protein complexes were eluted in DNA loading buffer (0.1% SDS, 5% glycerol and 0.005% bromophenol blue) by incubation at 50°C for 20 min. The bound DNA was analyzed by 1.5% agarose gel electrophoresis in 1× TAE and visualized with SYBR-Green I (Invitrogen). The amount of bound DNA was measured by quantifying the intensity of the bands using a FluorImager 595 (GE Healthcare) and ImageQuant software (Molecular Dynamics). Immunoprecipitation was performed three or six times. For negative controls, immunoprecipitation was performed without GST-Dnmt proteins.

Immunoblot and dot blot analysis

Protein samples in Laemmli's buffer (47) were resolved by SDS–PAGE and then transferred onto a PVDF or nitrocellulose membrane. For dot blot analysis, reconstituted chromatin arrays in 10 mM Tris–HCl (pH 7.5), 1 mM EDTA and 1 μg/μl BSA were spotted on a nitrocellulose membrane. Transferred or spotted membranes were probed with the following specific antibodies or antiserum, as indicated: anti-Dnmt3b and anti-Dnmt3a (1:50 000; provided by Dr E. Li) (55), anti-Dnmt3L (1:1000; provided by Dr S. Yamanaka) (30), anti-Dnmt3a (1:250; Imgenex IMG-268), anti-SirT1 (1:1000; Abcam ab12193), anti-HDAC1 (1:1000; Upstate 06-720), anti-HDAC2 (1:2000; Sigma H3159), anti-HP1α (1:1000; MBL BMP 001), anti-HP1β (1:1000; Euromedex 1MOD-1A9-As), anti-HP1γ (1:1000; Euromedex 2MOD-1G6-As), anti-PCNA (1:1000; Upstate 05-347), anti-Brg-1 (1:500; Santa Cruz sc-10768), anti-Lamin B1 (1:200; MBL JM-3046-3), anti-Oct-3/4 (1:250; Santa Cruz sc-9081), anti-FLAG (1:2000; Sigma F3165), anti-β-actin (1:1000; Sigma A2228), anti-Histone H3 lysine 9 tri-methylation (H3K9me3) (1:500; Abcam ab1186), anti-H3K9me2 (1:1000; Upstate 07-212), anti-H3K9me1 (1:1000; Abcam ab9045), anti-H4K20me3 (1:500; Abcam ab9053), anti-H4K20me1 (1:1000; Abcam ab8895), anti-H3K27me3 (1:1000; Upstate 07-449), anti-H3K4me3 (1:1000; Abcam ab8580), anti-acetyl lysine 9 Histone H3 (H3K9Ac) (1:1000; Upstate 06-942), anti-acetyl-Histone H3 (1:1000; Upstate 06-599), anti-H4K16Ac (1:1000; Upstate 07-329), anti-acetyl-Histone H4 (1:1000; Upstate 06-598), anti-Histone H3 (1:8000; Abcam ab1791), anti-Histone H4 (1:1000; Abcam ab10158) and anti-Histone H1 (1:250; Abcam ab7789). Immunoreactive proteins were visualized using Chemi Lumi One (Nacarai tesque) or ECL Plus (GE Healthcare).

Immunofluorescence

ES cells were cultured on collagen-treated cover slips (Becton, Dickinson and Company). For analysis, EB3 cells were transferred onto collagen-treated cover slips and cultured for 4 h. Cells were fixed with 4% paraformaldehyde in PBS for 10 min at room temperature. Fixed cells were washed with PBS and then

blocked in buffer (PBS containing 5 mg/ml BSA, 50 mM glycine, 2% goat serum and 0.1% sodium azide) for 30 min at room temperature. After blocking, cells were incubated overnight at 4°C with the following primary antibodies in blocking buffer, as indicated: anti-Dnmt3b (1:5000; provided by Dr E. Li) (55), anti-HP1α (1:500; Euromedex 2HP-1H5-As) and anti-Histone H1 (1:250; Abcam ab7789). After washing with PBS, cells were incubated with the following fluorescence-conjugated secondary antibodies in blocking buffer, as indicated: Alexa 546 anti-rabbit IgG (1:500; Invitrogen A-11035) and Alexa 488 anti-mouse IgG (1:500; Invitrogen A-11029). After washing with PBS, cells were counterstained with 0.5 mg/ml of 4′,6′-diamidino-2-phenylindole (DAPI). After washing in PBS and sterilized ultra pure water, coverslips were mounted with ProLong Gold (Invitrogen). Cells were analyzed using a Radiance 2100 laser scanning confocal microscope system (Bio-Rad) equipped with an inverted Nikon Eclipse TE-2000 microscope (Nikon) or Nikon A1 laser scanning confocal microscope system (Nikon) equipped with an inverted Nikon Eclipse Ti (Nikon).

Statistical analysis

Data represent the means with standard deviation (SD). The Student's *t*-test in the Stat View 5.0 software (SAS Institute Inc.) was used to calculate statistical significance.

RESULTS

Dnmt3b localizes to histone H1-enriched heterochromatin

To investigate the targeting mechanisms of *de novo* methyltransferases in the nucleus, we used ES cells, which express both *Dnmt3a* and *Dnmt3b* (55), and examined the expression of Dnmt3 proteins during ES cell differentiation. ES cells were cultured in suspension for 5 days in the absence of LIF to form EB, and then cells were plated in dishes for an additional 5 days to differentiate into primarily mesodermal cells. The expression of Oct3/4, a transcription factor essential for maintaining undifferentiated ES cells (56), decreased by 5 days after induction (Figure 1A) suggesting that differentiation had occurred. Dnmt3b and Dnmt3a2 were upregulated upon induction of ES cell differentiation, and then were gradually downregulated (Figure 1A). Dnmt3b and Dnmt3a2 were reduced in parallel with the reduction of Oct3/4 upon ES cell differentiation. In contrast to Dnmt3b and Dnmt3a2, Dnmt3a was expressed 8 days after induction. The amount of Dnmt3L gradually decreased as the ES cells differentiated. Since both Dnmt3b and Dnmt3a2 were highly expressed in early EB cells, Day 3 embryoid body (EB3) cells were used for further analysis of Dnmt3 proteins.

The subcellular distribution of Dnmt3b in EB3 cells was analyzed using a sequential extraction procedure (44) (Figure 1B). Fractionation efficiency was confirmed by the presence of PCNA in the nucleoplasm fraction that was readily extracted by detergent treatment, core histones in the chromatin fraction, and lamin B1 in the nuclear matrix fraction (Figure 1B). As previously reported, most Dnmt3b, Dnmt3a2 and Dnmt3L were found in the chromatin fraction in EB3 cells (30,37,55,57).

To further investigate the nuclear distribution of Dnmt3b in EB3 cells, we carried out biochemical fractionation using MNase. Isolated nuclei were subjected to MNase treatment in low salt buffer to generate transcriptionally active and inactive chromatin fractions (45,46). Nuclease treatment caused the initial release of mono- and oligonucleosomes, which predominantly contained transcriptionally active chromatin (S1 fraction). After the release of the S1 fraction, the resulting pellets were subjected to hypotonic lysis to release soluble polynucleosomes (S2 fraction). The S2 fraction was enriched in histone H1 and predominantly contained transcriptionally inactive chromatin. The remaining pellets contained the nuclear matrix (P fraction) (Figure 1C). Equivalent amounts of DNA from each fraction were subjected to electrophoresis, and then fluoro staining. As shown in Figure 1D, the S1 fraction was enriched in mononucleosomes, whereas the S2 and P fractions contained polynucleosomes. Nuclear proteins from equivalent amounts of chromatin DNA were separated by SDS–PAGE and then analyzed by immunoblot. Brg1, an ATPase subunit of chromatin-remodeling complexes, and HP1α were enriched in the S1 and P fractions, respectively (42). Dnmt3b and Dnmt3L were enriched in the S2 fraction, whereas Dnmt3a2 was present at equivalent levels in the S1 and S2 fractions (Figure 1E). Neither Dnmt3b, nor Dnmt3a2 accumulated in the P fraction, which is the major HP1α-containing fraction. Thus, biochemical fractionation revealed that Dnmt3b associated predominantly with nuclease-insensitive transcriptionally inactive chromatin, while Dnmt3a2 was distributed throughout the genome, independent of DNA accessibility.

Dnmt3b localizes to chromatin regions with histone H1 but not HP1α

To investigate the mechanism by which Dnmt3b recognizes target genomic sites for methylation, Dnmt3b complexes were purified from ES cells. An ES cell line that stably expressed a FLAG-epitope fused to Dnmt3b (FLAG-tagged Dnmt3b) was established to facilitate purification. Stable ES transformants exhibited <2-fold higher level of Dnmt3b in the undifferentiated and differentiated states (Figure 2A). Endogenous Dnmt3b in EB3 cells localized in the nucleus without forming intensely labeled foci. Results showed that the localization of FLAG-tagged Dnmt3b overlapped with that of endogenous Dnmt3b (Figure 2B and C). Consistent with the biochemical fractionation analysis of Dnmt3b (Figure 1E), nuclear localization of Dnmt3b more closely resembled that of linker histone H1 rather than HP1α, since the latter formed intensely-labeled foci that overlapped with DAPI-stained heterochromatic foci in ES and EB3 cells (Figures 1E, 2B, 2C and Supplementary Figure S1A and S1B).

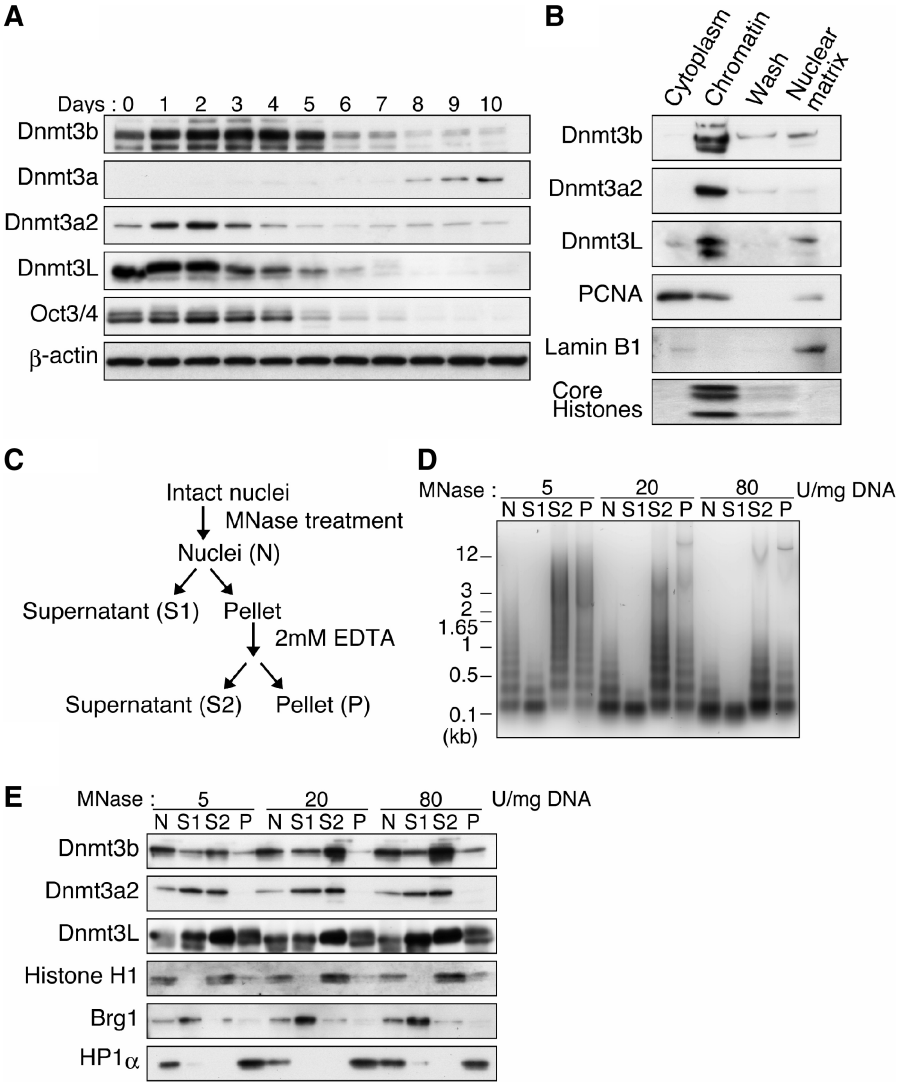

Figure 1. Dnmt3b is enriched in histone H1-containing chromatin fractions. (**A**) Dnmt3b, Dnmt3a2, Dnmt3a, Dnmt3L and Oct3/4 expression during ES cell differentiation. Equal amounts of protein (10 μg) from undifferentiated ES cells (Day 0) and differentiated ES cells (from Day 1 to 10) were analyzed by immunoblot using the indicated antibodies. (**B**) Subcellular distribution of Dnmt3b, Dnmt3a2 and Dnmt3L. ES cells were sequentially extracted to obtain cytoplasmic, chromatin and nuclear matrix fractions. Equal amounts of fractionated protein (10 μg) were separated by SDS–PAGE and then analyzed by immunoblot using the indicated antibodies. Fractionation efficiency was confirmed by immunoblot analysis using anti-PCNA (cytoplasm) and anti-lamin B1 (nuclear matrix) antibodies, and by Coomassie Brilliant Blue (CBB) staining of core histones (chromatin). (**C**) Schematic representation of chromatin fractionation. Isolated ES cell nuclei (N) were digested with 5, 20 or 80 U of MNase/mg DNA. Digested nuclei were fractionated into three fractions: transcriptionally active (S1), transcriptionally inactive (S2) and nuclear matrix-containing (P). (**D**) DNA samples from nuclear fractions N, S1, S2 and P. Equivalent amounts of DNA from each fraction were separated by 1.5% agarose gel electrophoresis in 1× TAE followed by SYBR-Green I staining. (**E**) Nuclear aliquots corresponding to 600 ng of DNA from N, S1, S2 and P fractions were separated by SDS–PAGE and then analyzed by immunoblot using the indicated antibodies.

Histone modifications in Dnmt3b associated chromatin

To further investigate the mechanism by which Dnmt3b recognizes target genomic sites for methylation, Dnmt3b-associated proteins were purified from FLAG-tagged Dnmt3b-expressing stable ES cells using immunoaffinity purification in 0.2 M NaCl (FLAG-IP). Nuclear extracts (S2 fraction, Figure 1E) were prepared in 0.4 M NaCl from MNase-treated FLAG-Dnmt3b-expressing ES cells. As a control, a mock purification from wild-type ES cells was performed and no associated proteins were detected by silver staining (Figure 3A). SDS–PAGE analysis of purified Dnmt3b complexes revealed that several polypeptides were specifically associated with FLAG-Dnmt3b. Through analysis of the associated polypeptides by LC/MS/MS, a 75 kDa Dnmt3b-associated protein, Dnmt3a2, was identified (Figure 3A). Six protein bands that corresponded to the sizes of core histones and histone H1 were also detected (Figure 3A). Consistent with a previous report (58), immunoblot analysis confirmed that Dnmt3b associated with Dnmt3a2 and with Dnmt3L even under 0.4 M NaCl extraction conditions (Figure 3B). HP1 proteins, which were not extracted in the S2 fraction under hypotonic conditions (Figure 1E), dissociated from chromatin under high

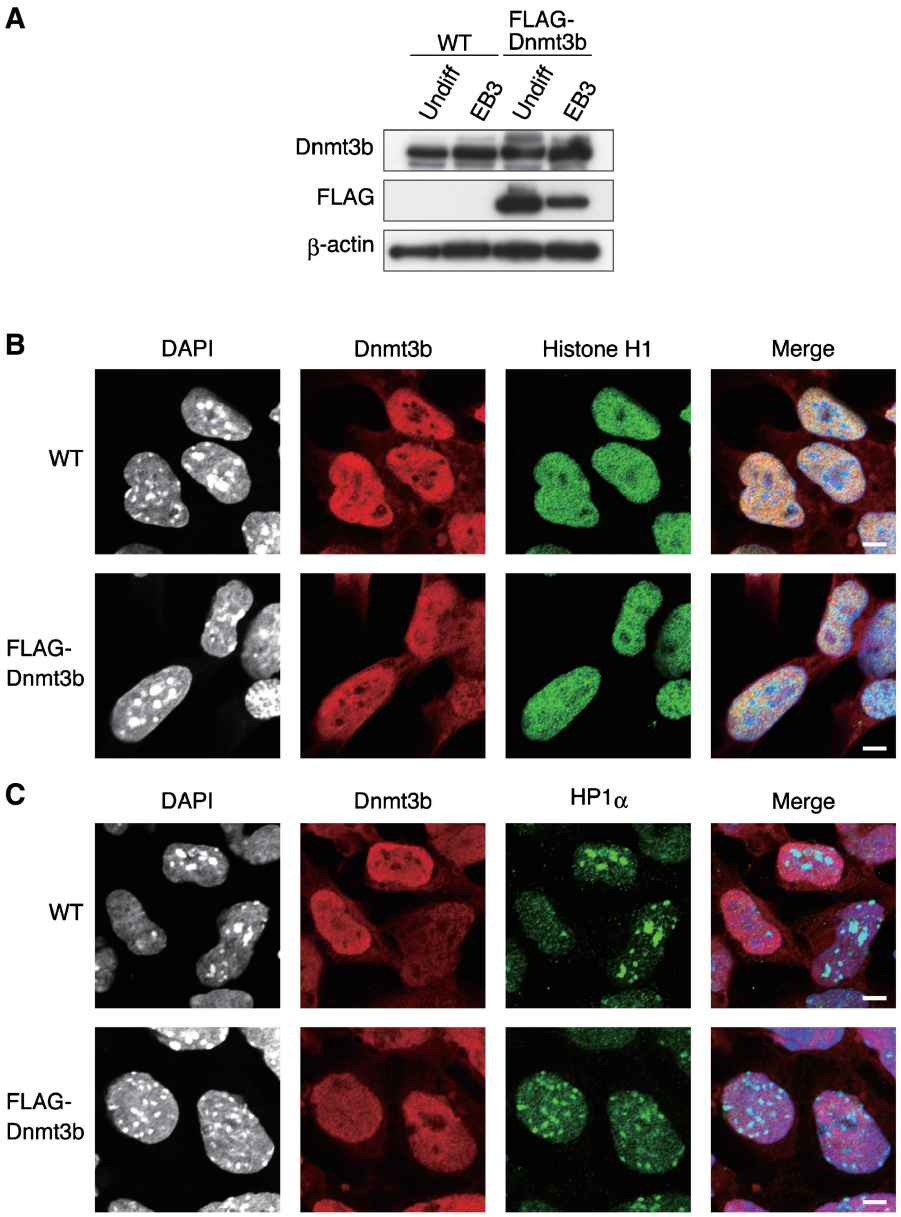

Figure 2. Establishment of a FLAG-Dnmt3b expressing cell line. (**A**) Expression of endogenous Dnmt3b and FLAG-Dnmt3b in undifferentiated (Undiff) and differentiated (EB3) ES cells. Total protein (4 μg) from parental wild-type ES cells (WT) and FLAG-Dnmt3b-expressing ES cells (FLAG-Dnmt3b) was analyzed by immunoblot using anti-Dnmt3b, anti-FLAG, and anti-β-actin antibodies. (**B**) Nuclear colocalization of Dnmt3b and histone H1 in EB3 cells. Parental ES cells (WT) and FLAG-Dnmt3b-expressing ES cells were immunostained with anti-Dnmt3b (red) or anti-histone H1 (green) antibodies. The cells were counterstained with DAPI (blue in the merged image). Endogenous Dnmt3b and exogenously-expressed FLAG-tagged Dnmt3b exhibited similar localization patterns. (**C**) Nuclear localization of Dnmt3b and HP1α in EB3 cells. Parental ES cells and FLAG-Dnmt3b-expressing cells were analyzed by immunofluorescence using anti-Dnmt3b (red) or anti-HP1α (green) antibodies. The cells were counterstained with DAPI (blue in the merged image). Scale bars, 5 μm.

salt conditions (37) and were present in the 0.4 M NaCl extracted S2 fractions. Interactions between Dnmt3b and HP1 proteins in 0.4 M NaCl extracted S2 fractions were not detected (Figure 3B).

In mammals, the silent heterochromatic status is associated with hypoacetylation of histones and specific histone methylation (59–61). To determine whether Dnmt3b recognized specific histone modifications, FLAG-Dnmt3b-associated core histones in the S2 fraction containing 75 mM NaCl were subjected to immunoblot analysis using methylation-specific histone H3 antibodies. Non-specific precipitation of core histones during purification of Dnmt3b-associated chromatin was evaluated by a mock purification with parental wild-type ES cells (Supplementary Figure S2A). Immunoblot analysis using an antibody against the globular domain of histone H3 served as a loading control between bulk chromatin and Dnmt3b-associated chromatin (32,62). As previously observed in Dnmt3L-associated chromatin (32), H3K4me3 was reduced in immunopurified

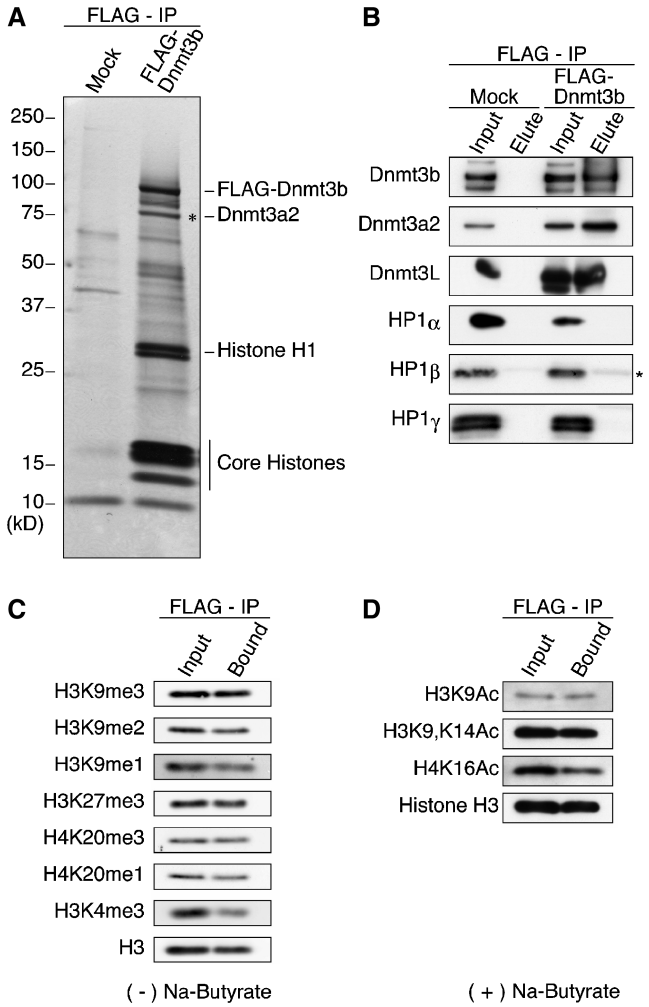

Figure 3. Dnmt3b stably associates with histone H1-containing chromatin in ES cells. (**A**) Silver staining of Dnmt3b-associated proteins purified from wild-type (Mock) or FLAG-Dnmt3b-expressing EB3 cells (FLAG-Dnmt3b). Dnmt3b-associated proteins were analyzed by immunoprecipitation in the presence of 0.2 M NaCl. Immunopurified FLAG-Dnmt3b-associated proteins were separated by 10–20% SDS–PAGE and then visualized by silver staining. LC/MS/MS spectra identified the 75 kDa Dnmt3b-associated protein (asterisk) as Dnmt3a2. Nuclear histones, including histone H1, also stably associated with Dnmt3b. (**B**) Dnmt3b-associated proteins were analyzed by immunoprecipitation in the presence of 0.4 M NaCl, followed by immunoblot using the indicated antibodies. Non-specific bands corresponding to the IgG light chain of the FLAG antibody were detected with the anti-HP1β antibody (asterisk). Input represents 20% of the nuclear extract used in the assay. (**C**) H3K4me3 was reduced in Dnmt3b-associated chromatin. Dnmt3b-associated chromatin was subjected to immunoblot analysis using antibodies that detected modified histones. Input represents 2.5% of the nuclear extract used in the assay. (**D**) H4K16Ac was reduced in Dnmt3b-associated chromatin. Dnmt3b-associated chromatin was subjected to immunoblot analysis using antibodies that detected modified histones. To analyze acetylated histones, nuclear extracts and immunoprecipitates were prepared in the presence of the histone deacetylase inhibitor Na butyrate. Input represents 4% of the nuclear extract used in the assay.

FLAG-Dnmt3b-associated chromatin (Figure 3C and Supplementary Figure S2B). H3K9me1, which is positively correlated with gene expression (59,63), was also slightly reduced in the Dnm3b-bound chromatin (Figure 3C). In contrast, little enrichment of silent chromatin-specific modifications, such as H3K9me3, H3K9me2, H3K27me3, H4K20me3 and H4K20me1 was detected (59,61) (Figure 3C and Supplementary Figure S2B). We further analyzed the effects of histone acetylation on Dnmt3b-binding in the S2 fraction prepared with sodium butyrate. As shown in Figure 3D, the level of H4K16Ac was relatively reduced in Dnmt3b-associated chromatin (Figure 3D). Acetylation of H4K16 induces decondensation of chromatin structures *in vitro* (64,65). These results suggested that Dnmt3b recognized condensed chromatin structures, rather than specific histone modifications.

Dnmt3b preferentially associates with nuclease-resistant higher-order chromatin in the nucleus

To characterize Dnmt3b-associated chromatin in ES cell nuclei, the interaction between Dnmt3b and chromatin was examined by treating nuclei with different concentrations of MNase. When ES cell nuclei were treated with 5 U/mg MNase, the chromatin was partially digested, whereas most chromatin was digested into mononucleosomes with 80 U/mg MNase (Figure 4A). After MNase treatment, nuclear extracts were subjected to immunoprecipitation using an anti-FLAG antibody to analyze the Dnmt3b–chromatin interaction. The interaction between Dnmt3b and chromatin was disrupted when ES cell nuclei were treated with 80 U/mg MNase (Figure 4B). Sucrose gradient centrifugation was used to further investigate Dnmt3b-associated chromatin. Soluble chromatin in the S2 fraction was subjected to 10–30% (w/v) sucrose gradient sedimentation under physiological salt conditions (75 mM NaCl), which maintains higher-order chromatin structures (66,67). Fractionated nucleosomal DNA was separated by 1.5% agarose gel electrophoresis and then visualized by fluoro staining as well as immunoblot analysis. Dnmt3b was enriched in histone H1-containing long chromatin fractions, and was not detected in shorter chromatin fractions (Figure 4C). These results suggested that Dnmt3b did not simply bind to DNA, but preferentially associated with higher-order chromatin.

Dnmt3b preferentially associates with higher-order reconstituted chromatin

To investigate the effects of chromatin structure on Dnmt3b binding, the binding affinity of Dnmt3b for differentially reconstituted nucleosomal DNA substrates was determined. Recombinant GST-Dnmt3a2 and GST-Dnmt3b fusion proteins were expressed in *E. coli* and purified (Figure 5A). We reconstituted mononucleosomes, 4-mer nucleosomes and 12-mer nucleosomal arrays on tandem 208 bp DNA repeats of the CpG rich 601 nucleosome positioning sequence (Figure 5B and Supplementary Figure S3) (49). Reconstituted chromatin or naked DNA was mixed with purified GST-Dnmt3b or GST-Dnmt3a2 at a molar ratio of one recombinant protein molecule per nucleosome core, and then protein-bound DNA was immunoprecipitated using an anti-GST antibody. Bound DNA was analyzed to quantify Dnmt3 binding, and the

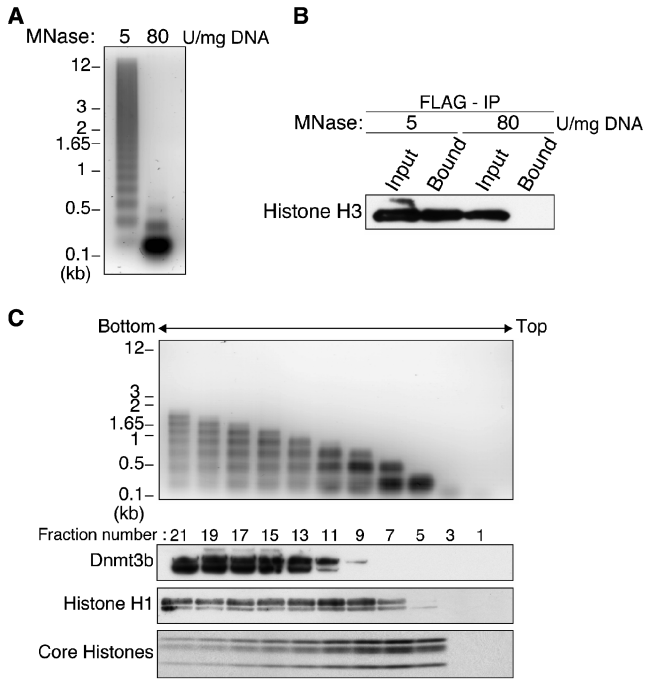

Figure 4. Dnmt3b associates with nuclease-resistant heterochromatin and the association requires higher-order chromatin structure. (**A**) DNA from nuclei digested with 5 or 80 U MNase/mg DNA. Equivalent amounts of DNA were separated by 1.5% agarose gel electrophoresis in 1× TAE and then visualized with SYBR-green I. (**B**) Detection of chromatin in FLAG-Dnmt3b immunoprecipitates. Nuclear extracts were digested with 5 or 80 U MNase/mg DNA, and subjected to immunoprecipitation using an anti-FLAG antibody in the presence of 75 mM NaCl. FLAG-Dnmt3b immunoprecipitates were analyzed by immunoblot using an anti-histone H3 antibody to confirm the interaction between Dnmt3b and chromatin. Input represents 4% of the nuclear extract used in the assay. (**C**) Dnmt3b co-sedimented with histone H1-containing poly-nucleosomes on a sucrose gradient. S2 fractions were subjected to 10–30% (w/v) sucrose gradient sedimentation. Equivalent aliquots of each DNA fraction and protein sample were analyzed by agarose gel electrophoresis and immunoblot using the indicated antibodies, respectively. Core histones in each fraction were visualized by CBB staining.

result was expressed as the percentage of the input DNA (Figure 5C and Supplementary Figures S4 and S5). The binding affinity of GST-Dnmt3b significantly increased with increasing numbers of nucleosomes in the reconstituted chromatin (Figure 5C). Furthermore, GST-Dnmt3b preferentially bound to nucleosomal 12×601 DNA as compared to naked 12×601 DNA (Figure 5C). In contrast to GST-Dnmt3b, GST-Dnmt3a2 bound weakly to all substrates regardless of DNA size or nucleosomal structure, and there were no significant differences in binding affinity among all substrates (Figure 5C). These results demonstrated that Dnmt3b preferentially associated with nucleosomal DNA rather than naked DNA, and suggested that the binding of Dnmt3b is dependent on chromatin structure.

Histone H1 binds near linker DNA between nucleosomes, and affects higher-order chromatin structure (68,69). Incorporation of histone H1 into reconstituted nucleosomal arrays induces a compaction of the chromatin fiber (70). To investigate whether Dnmt3b

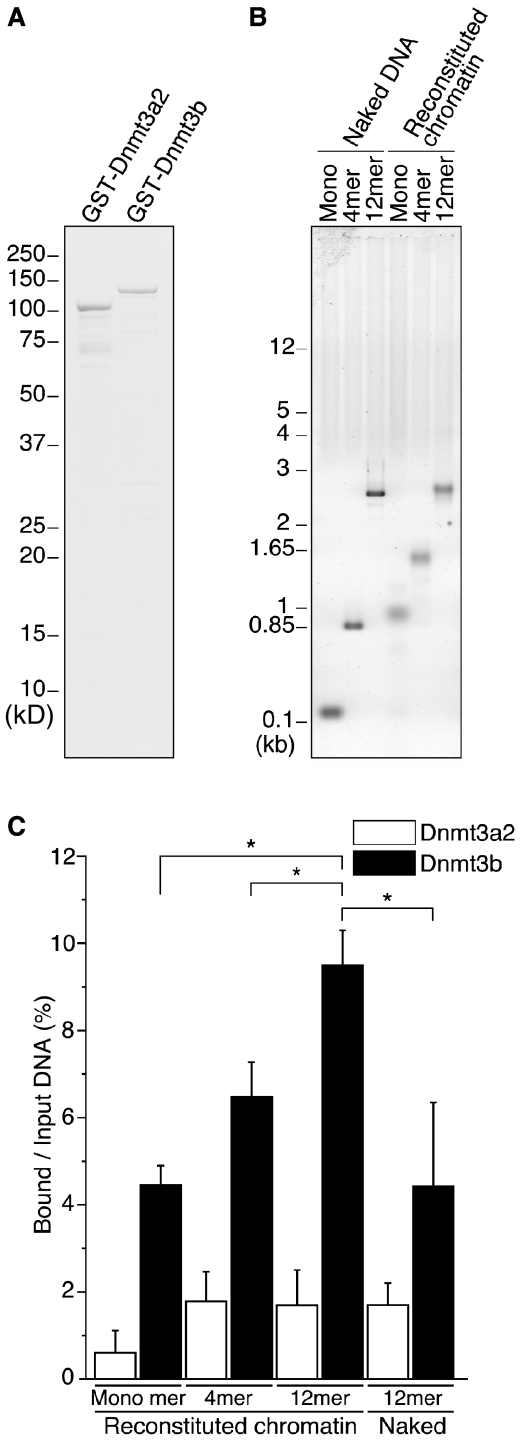

Figure 5. Dnmt3b preferentially binds to long chromatin *in vitro*. (**A**) Purified GST-Dnmt3a2 and GST-Dnmt3b. Purified protein was analyzed by 10–20% SDS–PAGE and then visualized by CBB staining. (**B**) Mononucleosomes, tetramers (4-mer) and 12-mer nucleosomal arrays (12-mer) were reconstituted into DNA templates containing 1, 4 and 12 tandem repeats of a 208 bp '601' sequence, respectively. Naked DNA templates and reconstituted chromatin were analyzed by 0.7% agarose gel electrophoresis. (**C**) Protein-bound DNA is expressed as a percentage of input DNA. Data represent the means with SD of three or six independent experiments (Supplementary Figure S5). The binding affinity of GST-Dnmt3b to 12-mer nucleosomal arrays was tested six times, while binding to the other three DNA templates was tested three times. Asterisk indicates a P-value of <0.05.

preferentially binds to highly folded chromatin, histone H1 was incorporated into reconstituted 12-mer nucleosomal arrays, and the effect was assessed by nucleoprotein agarose gel electrophoresis. When 12-mer arrays were incubated with increasing amounts of histone H1, a decrease in the migration of nucleoprotein complexes was found (Figure 6A). MNase digestion of histone H1-containing chromatin yielded chromatosomes, which confirmed that histone H1 was stably incorporated into the nucleosomal arrays (53) (Figure 6B). To estimate the relative amount of histone H1 to core histones, the reconstituted 12-mer nucleosomal arrays were precipitated with $MgCl_2$ (51). Precipitated material was separated by SDS–PAGE, and then subjected to SYPRO-Orange staining (Figure 6C and Supplementary Figure S6). The molar ratio of histone H1 to core histones was 0.53 at its maximum in the reconstituted chromatin (Figure 6D). In ES cells, the average ratio of histone H1 to core histones is approximately 0.46 (36). Thus, reconstituted nucleosomal arrays contained physiological amounts of histone H1. We next assessed the binding of GST-Dnmt3b to the reconstituted chromatin substrates (Supplementary Figures S4 and S7). As expected, the affinity of GST-Dnmt3b binding to chromatin increased with the incorporation of increasing amounts of histone H1 into the nucleosomal arrays (Figure 6E). These results suggested that Dnmt3b preferentially binds to higher-order chromatin structures.

Dnmt3b preferentially associates with hypoacetylated nucleosomal arrays *in vitro*

Histone acetylation neutralizes the net charge of lysine, reduces chromatin–chromatin interactions, and is associated with decondensed transcriptionally active chromatin (71). Recent studies have shown that acetylation of histone H4K16 induces the disruption of condensed chromatin fibers *in vitro* (64,65). To investigate the effect of histone acetylation on chromatin binding of Dnmt3b, hypo- and hyperacetylated nucleosomal arrays were prepared. When nucleosomal arrays are properly and fully positioned, monomer-sized nucleosomes are observed following the digestion of Sca I restriction sites in the linker DNA of 601 sequences between nucleosomes (50). We detected monomer-sized nucleosomes without naked DNA fragments by gel mobility shift analysis (Figure 7A, lanes 3–5), which indicated that the hypo- and hyperacetylated nucleosomal arrays were properly positioned and fully reconstituted (Figure 7A, lanes 6, 7 and Supplementary Figure S3). The level of histone acetylation in these nucleosomal arrays was analyzed by dot blot analysis. There was an enrichment of histone acetylation in hyperacetylated nucleosomal arrays (Figure 7B). To characterize any structural differences between the nucleosomal arrays, the sedimentation velocity was determined by analytical ultracentrifugation. In 2.5 mM NaCl without $MgCl_2$, hyperacetylated nucleosomal arrays had $S_{20,w}$ values of approximately 33S, while hypoacetylated nucleosomal arrays sedimented at approximately 38S. These results indicated that hypoacetylated nucleosomal arrays had a more compact chromatin structure than hyperacetylated nucleosomal arrays (Figure 7C). Using these two different nucleosomal arrays, a Dnmt3b binding assay was performed (Supplementary Figures S4 and S8). As shown in Figure 7D, Dnmt3b preferentially associated with the more condensed, hypoacetylated nucleosomal arrays. Consistent with the reduced amount of H4K16Ac in Dnmt3b-associated chromatin (Figure 3D), the amount of H4K16Ac was also reduced in GST-Dnmt3b associated chromatin (Supplementary Figure S9). These results prompted investigation into whether Dnmt3b associated with histone deacetylases in the nucleus. Co-immunoprecipitation analysis revealed that both the class I histone deacetylases HDAC 1/2 and the class III histone deacetylase SirT1 interact with Dnmt3b in the nuclease-insensitive S2 fraction under physiological salt conditions (75 mM NaCl) (Figure 7E, left). Specifically, interaction of Dnmt3b with SirT1, but not with HDAC1 or 2, was maintained even under high salt (0.4 M NaCl) conditions, indicating a stable interaction between them (Figure 7E, right). Recently co-localization of SirT1 and Dnmt3b was shown at a specific genomic region (72). Considering the preferential association of Dnmt3b with hypoacetylated nucleosomal arrays (Figure 7D), these results suggest that the deacetylation of histones by HDACs, including SirT1, promotes the recruitment of Dnmt3b into chromatin.

DISCUSSION

The results show that Dnmt3b in differentiated ES cells (EB3 cells) preferentially binds to nuclease-resistant condensed chromatin that contains linker histone H1 and histone deacetylases including SirT1, without a significant enrichment of silent-specific histone methylation. In addition, using reconstituted nucleosomal arrays as DNA substrates, Dnmt3b, but not Dnmt3a2, recognizes higher-order chromatin structures. Although further enzymatic analyses are required, the findings suggest that Dnmt3b is specifically recruited into condensed chromatin regions, recognizing higher-order chromatin structures, to stabilize gene silencing by DNA methylation.

During ES cell differentiation, the levels of Dnmt3b and Dnmt3a2 transiently increased and associated with chromatin (Figure 1A and B). Fractionation of chromatin by MNase treatment of EB3 cell nuclei revealed that Dnmt3b mainly associated with histone H1-containing condensed chromatin in the gene silent S2 fraction (Figure 1E). In contrast to Dnmt3b, Dnmt3a2 was found in both nuclease-sensitive S1 and insensitive S2 fractions equally (Figure 1E). Since the DNA-binding affinity of Dnmt3b increased significantly with increasing numbers of nucleosomes, while the binding of Dnmt3a2 was not affected by nucleosomal DNA structure (Figure 5C), Dnmt3a2 in the S2 fraction might associate with chromatin through interactions with Dnmt3b (Figure 3A and B).

A functional link between DNA methylation and histone H1, which contributes to higher order chromatin structure (69), has been demonstrated across the fungi, plant and animal kingdoms (35,36,73). Mouse ES cells

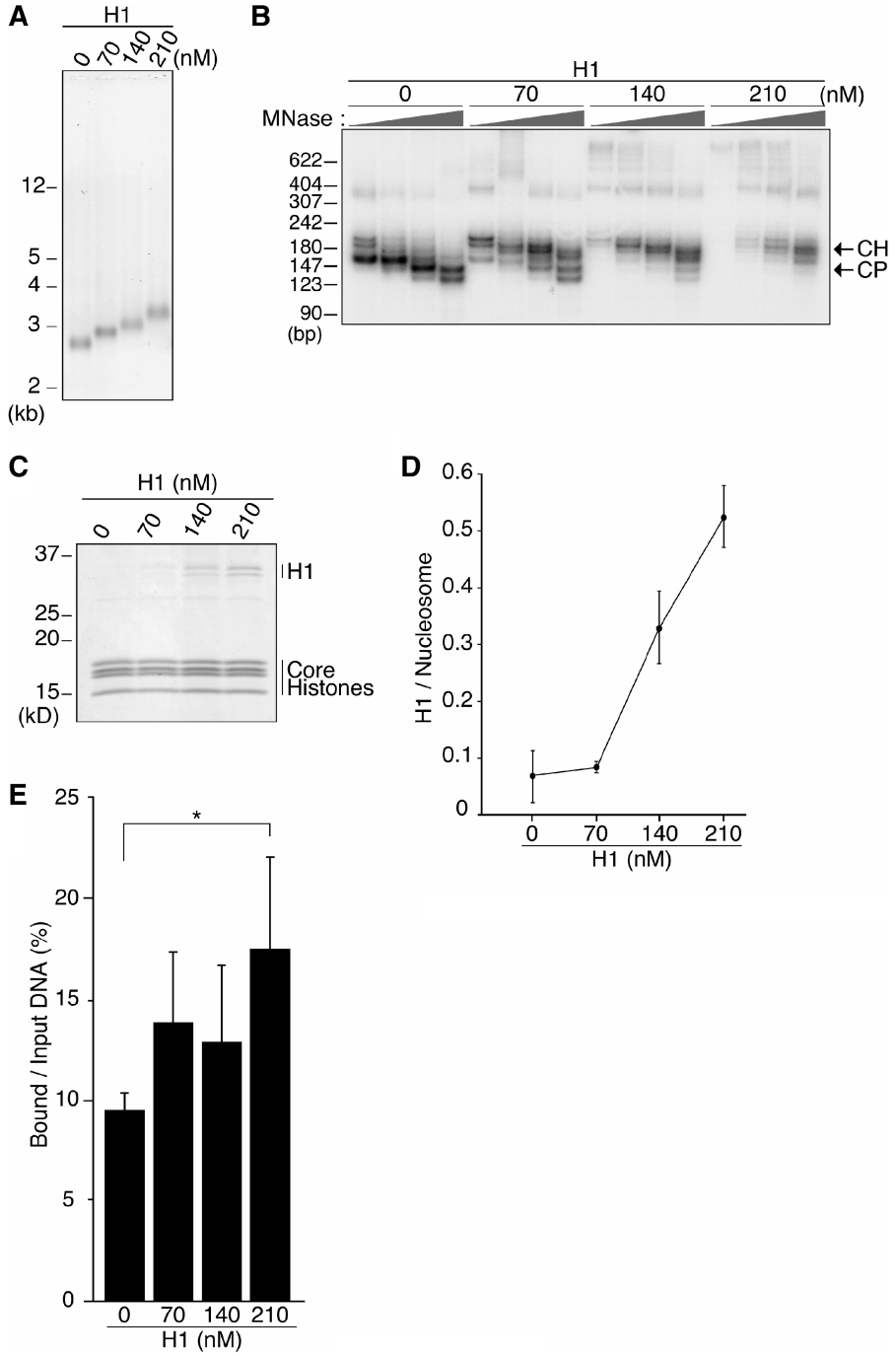

Figure 6. Dnmt3b preferentially binds to histone H1-assembled chromatin. (**A**) 12-mer nucleosomal arrays (70 nM nucleosome cores) were incubated with various amounts of histone H1 (0, 70, 140 or 210 nM). Binding of histone H1 to reconstituted chromatin was analyzed by 0.7% agarose gel electrophoresis. (**B**) MNase digestion of histone H1-containing 12-mer nucleosomal arrays. The reconstituted chromatin shown in A was digested with increasing amounts of MNase (0.141, 0.281, 0.562 and 1.125 U) as indicated by the triangles above the lanes. Products of digestion were labeled with [γ- ^{32} P]ATP and analyzed by native PAGE. Arrows indicate the positions of core particles (CP) and chromatosomes (CH). (**C**) Analysis of the protein component of the nucleosomal arrays. Reconstituted chromatin, as shown in A, was precipitated with $MgCl_2$, and subjected to 15–25% SDS–PAGE and visualized by SYPRO-orange staining (Supplementary Figure S6). (**D**) Data in C and Supplementary Figure S6 were quantified. The relative intensity of histone H1 to nucleosomes is shown as a solid line. Data represent the means with SD from three independent experiments. (**E**) The data in Supplementary Figure S7 were quantified, and are presented as a bar graph. Dnmt3b preferentially bound to histone H1-containing reconstituted 12-mers. Protein-bound DNA is expressed as a percentage of the input DNA. Data represent the means with SD of three or six independent experiments. The binding affinity of GST-Dnmt3b to 12-mer nucleosomal arrays (H1 = 0) was tested six times, while binding to the other three DNA templates was tested three times. Asterisk indicates a *P*-value of <0.05.

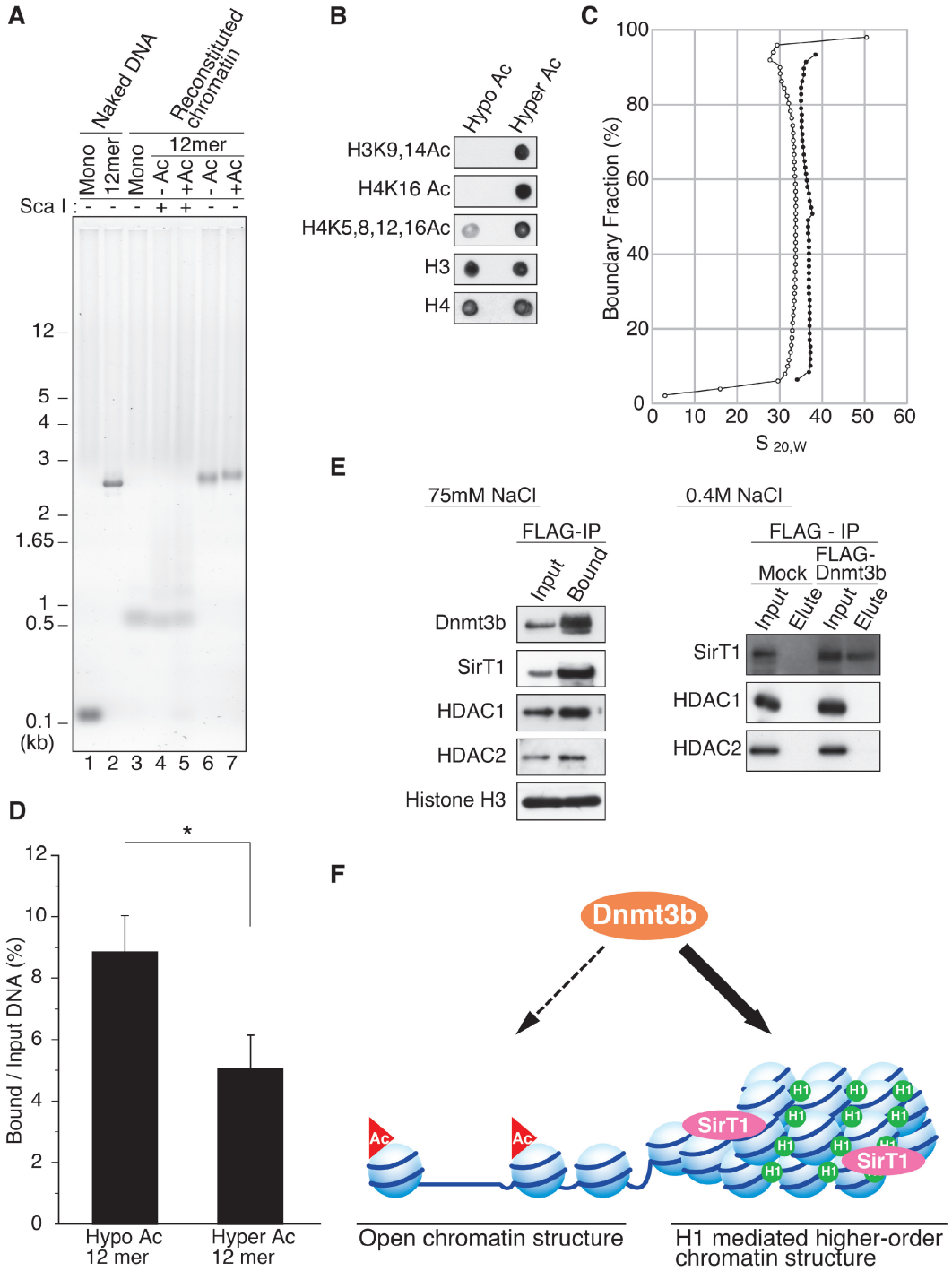

Figure 7. Dnmt3b preferentially associates with hypoacetylated chromatin *in vitro*. (**A**) Gel shift analysis of differentially acetylated 12-mer nucleosomal arrays. 12-mer arrays reconstituted with hypo- (−Ac) and hyper- (+Ac) acetylated core histones were analyzed by 0.7% agarose gel electrophoresis (lanes 6 and 7). Digestion of 12-mer nucleosomal arrays with Sca I produced mononucleosomes (lanes 4 and 5). Naked DNA of mononucleosomes, 12-mers and reconstituted mononucleosomes was analyzed as controls (lanes 1 to 3, respectively). (**B**) Acetylation levels of hypo- and hyperacetylated reconstituted 12-mer arrays were analyzed by dot-blot using the indicated antibodies. (**C**) Sedimentation coefficient distribution plots of hypoacetylated (closed circles) and hyperacetylated (open circles) 12-mer nucleosomal arrays. The percentage of the sample boundary measured by analytical ultracentrifugation is plotted against the sedimentation coefficient ($s_{20,w}$). (**D**) The data in Supplementary Figure S8 were quantified and are presented in bar graph form. Dnmt3b preferentially bound to hypoacetylated 12-mer nucleosomal arrays. The protein-bound DNA is expressed as a percentage of the input DNA. Data represent the means with SD of six independent experiments. Asterisk indicates a *P*-value of <0.01. (**E**) Dnmt3b associates with SirT1 in the ES cell nucleus. Dnmt3b-associated proteins were analyzed by immunoprecipitation in the presence of 75 mM or 0.4 M NaCl, followed by immunoblot using the indicated antibodies. Input represents 4% (75 mM NaCl) or 20% (0.4 M NaCl) of the nuclear extract used in the assay. (**F**) Hypothetical model for the stable association of Dnmt3b with chromatin for regional DNA methylation. Dnmt3b preferentially associates with condensed chromatin that contains histone H1 and SirT1. Red triangles and green circles represent acetylated histone and histone H1, respectively.

that lack three of six somatic histone H1 genes, in which the ratio of histone H1 to core histones is reduced from approximately 0.46 to 0.25, exhibit altered gene expression patterns and changes in DNA methylation (36). In the current study, the incorporation of histone H1 into reconstituted nucleosomal arrays (to over 0.5 H1 molecules per nucleosome core) significantly promoted chromatin binding of Dnmt3b (Figure 6E). Recent studies using long nucleosomal arrays showed that the incorporation of histone H1 induces a dose-dependent increase in chromatin compaction (64,70). The results suggest that Dnmt3b does not simply bind to DNA, but that it recognizes the condensed nucleosomal structure.

It was demonstrated previously that Dnmt3b associates with HP1α (25), which also contributes to the condensation of chromatin structures (74). HP1α was present predominantly in the nuclear matrix-containing nuclear pellet (P) fraction (Figure 1E) and the nuclear localization of Dnmt3b overlapped with that of histone H1, but not HP1α (Figure 2B and C). Dnmt3b was partially present in the P fraction besides the S2 fraction (Figure 1E), and the Dnmt3b in the P fraction appears to interact with HP1 proteins. The results indicate that most of the stable interactions of Dnmt3b with chromatin are independent of HP1α, as was also recently shown by sedimentation analysis (37).

Recent structural and biochemical studies demonstrated that the ADD domains of Dnmt3 proteins bind to histone H3 N-terminal tails that are unmethylated at lysine 4 (32–34). Consistent with this notion, Dnmt3b-bound chromatin was reduced for tri-methylated histone H3K4 in ES cells. In contrast, no significant accumulation of the inactive chromatin modifications H3K9me2/3, H3K27me3 or H4K20me3 in Dnmt3b-bound chromatin was found (Figure 3C and Supplementary Figure S2B). Furthermore, as shown in Figure 7D, histone deacetylation itself promoted Dnmt3b binding. The results suggest that histone deacetylation, rather than site-specific histone methylation, played an important role in the recruitment of Dnmt3b.

It has been shown that the N-terminus of histone H4 plays an important role in chromatin structure (50). Specifically, H4K16Ac induces the decondensation of reconstituted nucleosomal arrays, as determined by linker histone eviction (64,65). The reduction of histone H4K16Ac from Dnmt3b-bound chromatin (Figure 3D and Supplementary Figure S9) suggested that the physical interaction between Dnmt3b and chromatin was weakened by alterations in higher-order chromatin structures induced by acetylation of histone H4 at K16. In mammals, CpG islands within the 5′-promoter regions of many genes are usually unmethylated (62,75,76). These 5′-CpG islands are nuclease sensitive, reflecting histone hyperacetylation and nucleosome eviction (77–79). Dnmt3b exhibited a low preference for naked DNA (Figure 5C), and was enriched in the nuclease-insensitive S2 fraction (Figure 1E). Characterization of the Dnmt3b–chromatin interaction suggested that the chromatin environment of 5′-CpG islands is not suitable for the stable association of Dnmt3b with chromatin to induce DNA methylation.

The stable association of Dnmt3b with SirT1, which specifically deacetylates H4K16 (40), was found in the high salt S2 fraction (Figure 7E). In contrast, as recently reported (37), the interaction of Dnmt3b with HDAC1/2 (80–82) was disrupted in high-salt buffer (0.4 M NaCl). SirT1 is required for histone H1 recruitment in mammalian cells (39), and contributes to the onset of DNA methylation through the recruitment of DNMT3B to SIRT1-associated silent chromatin (72). It appears that SirT1 functions as a regulator of chromatin structure, creating a platform for the recruitment of Dnmt3b and subsequent DNA methylation (Figure 7F). Although additional studies are needed to elucidate the precise targeting mechanisms and enzymatic activity of Dnmt3b, the results suggest that Dnmt3b functions not only as a writer of DNA methylation but also as a molecular reader of condensed chromatin structure for further gene silencing.

SUPPLEMENTARY DATA

Supplementary Data are available at NAR Online.

ACKNOWLEDGEMENTS

We thank E. Li for the anti-Dnmt3a and anti-Dnmt3b serum; S. Yamanaka for the anti-Dnmt3L antibody; H. Niwa for the pCAGIpuro DNA; T. Richmond for the 601-208 × 12 DNA; M. Sakai for technical support with the sedimentation velocity analyses; I. Suetake, S. Tajima, C. Masutani and H. Kimura for technical advice; J. Goddi and H. Sasaki for valuable comments on the article and members of our laboratory for support and discussion.

FUNDING

Ministry of Education, Culture, Sports, Science and Technology of Japan, Grant-in-Aid for Scientific Research (grant numbers 19038015, 21114510, to K.U.); Japan Science and Technology Agency (JST) Precursory Research for Embryonic Science and Technology (PRESTO) program Osaka University for female researchers. Funding for open access charge: JST PRESTO program.

Conflict of interest statement. None declared.

REFERENCES

1. Robertson,K.D. and Wolffe,A.P. (2000) DNA methylation in health and disease. *Nat. Rev. Genet.*, **1**, 11–19.
2. Suzuki,M.M. and Bird,A. (2008) DNA methylation landscapes: provocative insights from epigenomics. *Nat. Rev. Genet.*, **9**, 465–476.
3. Hajkova,P., Erhardt,S., Lane,N., Haaf,T., El-Maarri,O., Reik,W., Walter,J. and Surani,M.A. (2002) Epigenetic reprogramming in mouse primordial germ cells. *Mech. Dev.*, **117**, 15–23.
4. Mayer,W., Niveleau,A., Walter,J., Fundele,R. and Haaf,T. (2000) Demethylation of the zygotic paternal genome. *Nature*, **403**, 501–502.
5. Santos,F., Hendrich,B., Reik,W. and Dean,W. (2002) Dynamic reprogramming of DNA methylation in the early mouse embryo. *Dev. Biol.*, **241**, 172–182.

6. Ehrlich,M., Gama-Sosa,M.A., Huang,L.H., Midgett,R.M., Kuo,K.C., McCune,R.A. and Gehrke,C. (1982) Amount and distribution of 5-methylcytosine in human DNA from different types of tissues of cells. *Nucleic Acids Res.*, **10**, 2709–2721.
7. Bourc'His,D. and Bestor,T.H. (2004) Meiotic catastrophe and retrotransposon reactivation in male germ cells lacking Dnmt3L. *Nature*, **430**, 96–99.
8. Hirasawa,R., Chiba,H., Kaneda,M., Tajima,S., Li,E., Jaenisch,R. and Sasaki,H. (2008) Maternal and zygotic Dnmt1 are necessary and sufficient for the maintenance of DNA methylation imprints during preimplantation development. *Genes Dev.*, **22**, 1607–1616.
9. Sado,T., Okano,M., Li,E. and Sasaki,H. (2004) De novo DNA methylation is dispensable for the initiation and propagation of X chromosome inactivation. *Development*, **131**, 975–982.
10. Bestor,T., Laudano,A., Mattaliano,R. and Ingram,V. (1988) Cloning and sequencing of a cDNA encoding DNA methyltransferase of mouse cells. The carboxyl-terminal domain of the mammalian enzymes is related to bacterial restriction methyltransferases. *J. Mol. Biol.*, **203**, 971–983.
11. Okano,M., Xie,S. and Li,E. (1998) Cloning and characterization of a family of novel mammalian DNA (cytosine-5) methyltransferases [1]. *Nat. Genet.*, **19**, 219–220.
12. Li,E., Bestor,T.H. and Jaenisch,R. (1992) Targeted mutation of the DNA methyltransferase gene results in embryonic lethality. *Cell*, **69**, 915–926.
13. Okano,M., Bell,D.W., Haber,D.A. and Li,E. (1999) DNA methyltransferases Dnmt3a and Dnmt3b are essential for de novo methylation and mammalian development. *Cell*, **99**, 247–257.
14. Cedar,H. and Bergman,Y. (2009) Linking DNA methylation and histone modification: patterns and paradigms. *Nat. Rev. Genet.*, **10**, 295–304.
15. De La Fuente,R., Baumann,C., Fan,T., Schmidtmann,A., Dobrinski,I. and Muegge,K. (2006) Lsh is required for meiotic chromosome synapsis and retrotransposon silencing in female germ cells. *Nat. Cell Biol.*, **8**, 1448–1454.
16. Gibbons,R.J., McDowell,T.L., Raman,S., O'Rourke,D.M., Garrick,D., Ayyub,H. and Higgs,D.R. (2000) Mutations in ATRX, encoding a SWI/SNF-like protein, cause diverse changes in the pattern of DNA methylation. *Nat. Genet.*, **24**, 368–371.
17. Wassenegger,M., Heimes,S., Riedel,L. and Sänger,H.L. (1994) RNA-directed de novo methylation of genomic sequences in plants. *Cell*, **76**, 567–576.
18. Strahl,B.D. and Allis,C.D. (2000) The language of covalent histone modifications. *Nature*, **403**, 41–45.
19. Taverna,S.D., Li,H., Ruthenburg,A.J., Allis,C.D. and Patel,D.J. (2007) How chromatin-binding modules interpret histone modifications: lessons from professional pocket pickers. *Nat. Struct. Mol. Biol.*, **14**, 1025–1040.
20. Vermeulen,M., Mulder,K.W., Denissov,S., Pijnappel,W.W.M.P., van Schaik,F.M.A., Varier,R.A., Baltissen,M.P.A., Stunnenberg,H.G., Mann,M. and Timmers,H.T.M. (2007) Selective anchoring of TFIID to nucleosomes by trimethylation of histone H3 lysine 4. *Cell*, **131**, 58–69.
21. Zhou,J., Fan,J.Y., Rangasamy,D. and Tremethick,D.J. (2007) The nucleosome surface regulates chromatin compaction and couples it with transcriptional repression. *Nat. Struct. Mol. Biol.*, **14**, 1070–1076.
22. Tamaru,H. and Selker,E.U. (2001) A histone H3 methyltransferase controls DNA methylation in Neurospora crassa. *Nature*, **414**, 277–283.
23. Tamaru,H., Zhang,X., McMillen,D., Singh,P.B., Nakayama,J.I., Grewal,S.I., Allis,C.D., Cheng,X. and Selker,E.U. (2003) Trimethylated lysine 9 of histone H3 is a mark for DNA methylation in Neurospora crassa. *Nat. Genet.*, **34**, 75–79.
24. Jackson,J.P., Lindroth,A.M., Cao,X. and Jacobsen,S.E. (2002) Control of CpNpG DNA methylation by the KRYPTONITE histone H3 methyltransferase. *Nature*, **416**, 556–560.
25. Lehnertz,B., Ueda,Y., Derijck,A.A.H.A., Braunschweig,U., Perez-Burgos,L., Kubicek,S., Chen,T., Li,E., Jenuwein,T. and Peters,A.H.F.M. (2003) Suv39h-mediated histone H3 lysine 9 methylation directs DNA methylation to major satellite repeats at pericentric heterochromatin. *Curr. Biol.*, **13**, 1192–1200.
26. Vire,E., Brenner,C., Deplus,R., Blanchon,L., Fraga,M., Didelot,C., Morey,L., Van Eynde,A., Bernard,D., Vanderwinden,J.M. *et al.* (2006) The Polycomb group protein EZH2 directly controls DNA methylation. *Nature*, **439**, 871–874.
27. Zhao,Q., Rank,G., Tan,Y.T., Li,H., Moritz,R.L., Simpson,R.J., Cerruti,L., Curtis,D.J., Patel,D.J., Allis,C.D. *et al.* (2009) PRMT5-mediated methylation of histone H4R3 recruits DNMT3A, coupling histone and DNA methylation in gene silencing. *Nat. Struct. Mol. Biol.*, **16**, 304–311.
28. Aapola,U., Kawasaki,K., Scott,H.S., Ollila,J., Vihinen,M., Heino,M., Shintani,A., Kawasaki,K., Minoshima,S., Krohn,K. *et al.* (2000) Isolation and initial characterization of a novel zinc finger gene, DNMT3L, on 21q22.3, related to the cytosine-5-methyltransferase 3 gene family. *Genomics*, **65**, 293–298.
29. Suetake,I., Shinozaki,F., Miyagawa,J., Takeshima,H. and Tajima,S. (2004) DNMT3L stimulates the DNA methylation activity of Dnmt3a and Dnmt3b through a direct interaction. *J. Biol. Chem.*, **279**, 27816–27823.
30. Nimura,K., Ishida,C., Koriyama,H., Hata,K., Yamanaka,S., Li,E., Ura,K. and Kaneda,Y. (2006) Dnmt3a2 targets endogenous Dnmt3L to ES cell chromatin and induces regional DNA methylation. *Genes. Cell*, **11**, 1225–1237.
31. Jia,D., Jurkowska,R.Z., Zhang,X., Jeltsch,A. and Cheng,X. (2007) Structure of Dnmt3a bound to Dnmt3L suggests a model for de novo DNA methylation. *Nature*, **449**, 248–251.
32. Ooi,S.K.T., Qiu,C., Bernstein,E., Li,K., Jia,D., Yang,Z., Erdjument-Bromage,H., Tempst,P., Lin,S.P., Allis,C.D. *et al.* (2007) DNMT3L connects unmethylated lysine 4 of histone H3 to de novo methylation of DNA. *Nature*, **448**, 714–717.
33. Otani,J., Nankumo,T., Arita,K., Inamoto,S., Ariyoshi,M. and Shirakawa,M. (2009) Structural basis for recognition of H3K4 methylation status by the DNA methyltransferase 3A ATRX-DNMT3-DNMT3L domain. *EMBO Rep.*, **10**, 1235–1241.
34. Zhang,Y., Jurkowska,R., Soeroes,S., Rajavelu,A., Dhayalan,A., Bock,I., Rathert,P., Brandt,O., Reinhardt,R., Fischle,W. *et al.* (2010) Chromatin methylation activity of Dnmt3a and Dnmt3a/3L is guided by interaction of the ADD domain with the histone H3 tail. *Nucleic Acids Res.*, **38**, 4246–4253.
35. Wierzbicki,A.T. and Jerzmanowski,A. (2005) Suppression of histone H1 genes in arabidopsis results in heritable developmental defects and stochastic changes in DNA methylation. *Genetics*, **169**, 997–1008.
36. Fan,Y., Nikitina,T., Zhao,J., Fleury,T.J., Bhattacharyya,R., Bouhassira,E.E., Stein,A., Woodcock,C.L. and Skoultchi,A.I. (2005) Histone H1 depletion in mammals alters global chromatin structure but causes specific changes in gene regulation. *Cell*, **123**, 1199–1212.
37. Jeong,S., Liang,G., Sharma,S., Lin,J.C., Choi,S.H., Han,H., Yoo,C.B., Egger,G., Yang,A.S. and Jones,P.A. (2009) Selective anchoring of DNA methyltransferases 3A and 3B to nucleosomes containing methylated DNA. *Mol. Cell. Biol.*, **29**, 5366–5376.
38. Takeshima,H., Suetake,I., Shimahara,H., Ura,K., Tate,S.I. and Tajima,S. (2006) Distinct DNA methylation activity of Dnmt3a and Dnmt3b towards naked and nucleosomal DNA. *J. Biochem.*, **139**, 503–515.
39. Vaquero,A., Scher,M., Lee,D., Erdjument-Bromage,H., Tempst,P. and Reinberg,D. (2004) Human SirT1 interacts with histone H1 and promotes formation of facultative heterochromatin. *Mol. Cell.*, **16**, 93–105.
40. Vaquero,A., Sternglanz,R. and Reinberg,D. (2007) NAD^+-dependent deacetylation of H4 lysine 16 by class III HDACs. *Oncogene*, **26**, 5505–5520.
41. Ishida,C., Ura,K., Hirao,A., Sasaki,H., Toyoda,A., Sakaki,Y., Niwa,H., Li,E. and Kaneda,Y. (2003) Genomic organization and promoter analysis of the Dnmt3b gene. *Gene*, **310**, 151–159.
42. Remboutsika,E., Lutz,Y., Gansmuller,A., Vonesch,J.L., Losson,R. and Chambon,P. (1999) The putative nuclear receptor mediator TIF1alpha is tightly associated with euchromatin. *J. Cell Sci.*, **112**, 1671–1683.
43. Ura,K. and Kaneda,Y. (2001) Reconstitution of chromatin in vitro. *Methods Mol. Biol.*, **181**, 309–325.
44. He,D., Nickerson,J.A. and Penman,S. (1990) Core filaments of the nuclear matrix. *J. Cell Biol.*, **110**, 569–580.
45. Huang,S.Y. and Garrard,W.T. (1989) Electrophoretic analyses of nucleosomes and other protein-DNA complexes. *Methods Enzymol.*, **170**, 116–142.

46. Rose,S.M. and Garrard,W.T. (1984) Differentiation-dependent chromatin alterations precede and accompany transcription of immunoglobulin light chain genes. *J. Biol. Chem.*, **259**, 8534–8544.
47. Laemmli,U.K. (1970) Cleavage of structural proteins during the assembly of the head of bacteriophage T4. *Nature*, **227**, 680–685.
48. Aoki,A., Suetake,I., Miyagawa,J., Fujio,T., Chijiwa,T., Sasaki,H. and Tajima,S. (2001) Enzymatic properties of the de novo-type mouse DNA (cytosine-5) methyltransferases. *Nucleic Acids Res.*, **29**, 3506–3512.
49. Lowary,P.T. and Widom,J. (1998) New DNA sequence rules for high affinity binding to histone octamer and sequence-directed nucleosome positioning. *J. Mol. Biol.*, **276**, 19–42.
50. Dorigo,B., Schalch,T., Bystricky,K. and Richmond,T.J. (2003) Chromatin fiber folding: Requirement for the histone H4 N-terminal tail. *J. Mol. Biol.*, **327**, 85–96.
51. Huynh,V.A.T., Robinson,P.J.J. and Rhodes,D. (2005) A method for the in vitro reconstitution of a defined "30 nm" chromatin fibre containing stoichiometric amounts of the linker histone. *J. Mol. Biol.*, **345**, 957–968.
52. Schwarz,P.M., Felthauser,A., Fletcher,T.M. and Hansen,J.C. (1996) Reversible oligonucleosome self-association: dependence on divalent cations and core histone tail domains. *Biochemistry*, **35**, 4009–4015.
53. Ura,K., Hayes,J.J. and Wolffe,A.P. (1995) A positive role for nucleosome mobility in the transcriptional activity of chromatin templates: restriction by linker histones. *EMBO J.*, **14**, 3752–3765.
54. Carruthers,L.M., Bednar,J., Woodcock,C.L. and Hansen,J.C. (1998) Linker histones stabilize the intrinsic salt-dependent folding of nucleosomal arrays: mechanistic ramifications for higher-order chromatin folding. *Biochemistry*, **37**, 14776–14787.
55. Chen,T., Ueda,Y., Xie,S. and Li,E. (2002) A novel Dnmt3a isoform produced from an alternative promoter localizes to euchromatin and its expression correlates with active de novo methylation. *J. Biol. Chem.*, **277**, 38746–38754.
56. Niwa,H., Miyazaki,J.I. and Smith,A.G. (2000) Quantitative expression of Oct-3/4 defines differentiation, dedifferentiation or self-renewal of ES cells. *Nat. Genet.*, **24**, 372–376.
57. Ge,Y.-Z., Pu,M.-T., Gowher,H., Wu,H.-P., Ding,J.-P., Jeltsch,A. and Xu,G.-L. (2004) Chromatin targeting of de novo DNA methyltransferases by the PWWP Domain. *J. Biol. Chem.*, **279**, 25447–25454.
58. Li,J.-Y., Pu,M.-T., Hirasawa,R., Li,B.-Z., Huang,Y.-N., Zeng,R., Jing,N.-H., Chen,T., Li,E., Sasaki,H. *et al.* (2007) Synergistic function of DNA methyltransferases Dnmt3a and Dnmt3b in the methylation of Oct4 and Nanog. *Mol. Cell Biol.*, **27**, 8748–8759.
59. Barski,A., Cuddapah,S., Cui,K., Roh,T.Y., Schones,D.E., Wang,Z., Wei,G., Chepelev,I. and Zhao,K. (2007) High-resolution profiling of histone methylations in the human genome. *Cell*, **129**, 823–837.
60. Grunstein,M. (1997) Histone acetylation in chromatin structure and transcription. *Nature*, **389**, 349–352.
61. Mikkelsen,T.S., Ku,M., Jaffe,D.B., Issac,B., Lieberman,E., Giannoukos,G., Alvarez,P., Brockman,W., Kim,T.K., Koche,R.P. *et al.* (2007) Genome-wide maps of chromatin state in pluripotent and lineage-committed cells. *Nature*, **448**, 553–560.
62. Thomson,J.P., Skene,P.J., Selfridge,J., Clouaire,T., Guy,J., Webb,S., Kerr,A.R., Deaton,A., Andrews,R., James,K.D. *et al.* (2010) CpG islands influence chromatin structure via the CpG-binding protein Cfp1. *Nature*, **464**, 1082–1086.
63. Cui,K., Zang,C., Roh,T.Y., Schones,D.E., Childs,R.W., Peng,W. and Zhao,K. (2009) Chromatin signatures in multipotent human hematopoietic stem cells indicate the fate of bivalent genes during differentiation. *Cell Stem Cell*, **4**, 80–93.
64. Robinson,P.J.J., An,W., Routh,A., Martino,F., Chapman,L., Roeder,R.G. and Rhodes,D. (2008) 30 nm chromatin fibre decompaction requires both H4-K16 acetylation and linker histone eviction. *J. Mol. Biol.*, **381**, 816–825.
65. Shogren-Knaak,M., Ishii,H., Sun,J.M., Pazin,M.J., Davie,J.R. and Peterson,C.L. (2006) Histone H4-K16 acetylation controls chromatin structure and protein interactions. *Science*, **311**, 844–847.
66. Allan,J., Cowling,G.J., Harborne,N., Cattini,P., Craigie,R. and Gould,H. (1981) Regulation of the higher-order structure of chromatin by histones H1 and H5. *J. Cell Biol.*, **90**, 279–288.
67. Thoma,F., Koller,T. and Klug,A. (1979) Involvement of histone H1 in the organization of the nucleosome and of the salt-dependent superstructures of chromatin. *J. Cell Biol.*, **83**, 403–427.
68. Bednar,J., Horowitz,R.A., Grigoryev,S.A., Carruthers,L.M., Hansen,J.C., Koster,A.J. and Woodcock,C.L. (1998) Nucleosomes, linker DNA, and linker histone form a unique structural motif that directs the higher-order folding and compaction of chromatin. *Proc. Natl Acad. Sci. USA*, **95**, 14173–14178.
69. Saeki,H., Ohsumi,K., Aihara,H., Ito,T., Hirose,S., Ura,K. and Kaneda,Y. (2005) Linker histone variants control chromatin dynamics during early embryogenesis. *Proc. Natl Acad. Sci. USA*, **102**, 5697–5702.
70. Routh,A., Sandin,S. and Rhodes,D. (2008) Nucleosome repeat length and linker histone stoichiometry determine chromatin fiber structure. *Proc. Natl Acad. Sci. USA*, **105**, 8872–8877.
71. Sperling,A.S. and Grunstein,M. (2009) Histone H3 N-terminus regulates higher order structure of yeast heterochromatin. *Proc. Natl Acad. Sci. USA*, **106**, 13153–13159.
72. O'Hagan,H.M., Mohammad,H.P. and Baylin,S.B. (2008) Double strand breaks can initiate gene silencing and SIRT1-dependent onset of DNA methylation in an exogenous promoter CpG island. *PLoS Genet.*, **4**, art. no. e1000155.
73. Barra,J.L., Rhounim,L., Rossignol,J.L. and Faugeron,G. (2000) Histone H1 is dispensable for methylation-associated gene silencing in Ascobolus immersus and essential for long life span. *Mol. Cell. Biol.*, **20**, 61–69.
74. Fan,J.Y., Rangasamy,D., Luger,K. and Tremethick,D.J. (2004) H2A.Z alters the nucleosome surface to promote HP1α-mediated chromatin fiber folding. *Mol. Cell*, **16**, 655–661.
75. Eckhardt,F., Lewin,J., Cortese,R., Rakyan,V.K., Attwood,J., Burger,M., Burton,J., Cox,T.V., Davies,R., Down,T.A. *et al.* (2006) DNA methylation profiling of human chromosomes 6, 20 and 22. *Nat. Genet.*, **38**, 1378–1385.
76. Weber,M., Hellmann,I., Stadler,M.B., Ramos,L., Pääbo,S., Rebhan,M. and Schübeler,D. (2007) Distribution, silencing potential and evolutionary impact of promoter DNA methylation in the human genome. *Nat. Genet.*, **39**, 457–466.
77. Ramirez-Carrozzi,V.R., Braas,D., Bhatt,D.M., Cheng,C.S., Hong,C., Doty,K.R., Black,J.C., Hoffmann,A., Carey,M. and Smale,S.T. (2009) A unifying model for the selective regulation of inducible transcription by CpG islands and nucleosome remodeling. *Cell*, **138**, 114–128.
78. Roh,T.Y., Cuddapah,S. and Zhao,K. (2005) Active chromatin domains are defined by acetylation islands revealed by genome-wide mapping. *Genes Dev.*, **19**, 542–552.
79. Tazi,J. and Bird,A. (1990) Alternative chromatin structure at CpG islands. *Cell*, **60**, 909–920.
80. Bachman,K.E., Rountree,M.R. and Baylin,S.B. (2001) Dnmt3a and Dnmt3b are transcriptional repressors that exhibit unique localization properties to heterochromatin. *J. Biol. Chem.*, **276**, 32282–32287.
81. Geiman,T.M., Sankpal,U.T., Robertson,A.K., Zhao,Y., Zhao,Y. and Robertson,K.D. (2004) DNMT3B interacts with hSNF2H chromatin remodeling enzyme, HDACs 1 and 2, and components of the histone methylation system. *Biochem. Biophys. Res. Commun.*, **318**, 544–555.
82. Bai,S., Ghoshal,K., Datta,J., Majumder,S., Yoon,S.O. and Jacob,S.T. (2005) DNA methyltransferase 3b regulates nerve growth factor-induced differentiation of PC12 cells by recruiting histone deacetylase 2. *Mol. Cell Biol.*, **25**, 751–766.